Instructions for use

Cytotoxicity of Lead Quantum Dots Due to Photochemical and Interfacial Degradation

Philip Jones,[1,2,†] Sobhanan Jeladhara,[3,†] Reiko Kohara,[3] Sakiko Sugino,[1] Martin Vacha,[4] Yuta Takano,[2,3,*] Fred Lacy,[2,5] Vasudevanpillai Biju[1,2,3,*]

[1]Health Research Institute, National Institute of Advanced Industrial Science and Technology (AIST), 2217-14 Hayashi-Cho, Takamatsu, Kagawa 7601-0369, Japan, and [2]Department of Environmental Toxicology, Southern University, Baton Rouge, LA 70813, USA, [3]Research Institute for Electronic Science, Hokkaido University, Sapporo, Hokkaido 001-0020, JAPAN, [4]Department of Materials Science and Engineering, Tokyo Institute of Technology, Ookayama 2-12-1-S8-44, Meguro-ku, Tokyo 152-8552, Japan, and [5]Department of Electrical Engineering, Southern University, Baton Rouge, LA 70813, USA

[†]Equal first author
Email: tak@es.hokudai.ac.jp, biju@es.hokudai.ac.jp,

Abstract

The increased production of heavy metal-based nanomaterials such as quantum dots and perovskites nanocrystals for energy harvesting, optoelectronic devices, bioanalysis, phototherapy and consumer health products rises concerns on the release of heavy metal ions into the environment. After disposal, these products may be degraded by interaction with the environment, such as rain, surface waters, soil and moisture, as well as solar irradiation, leading to the release of heavy metal ions into the environment with exposure to aquatic animals, surface waters and groundwater aquifers, further contaminating sources of clean drinking water. Researchers are in the early stages of understanding the potential toxicity of such nanomaterials and quantifying the amount of metal ions released due to environmental or biological transformation. Here we evaluate the toxicity of environmentally transformed nanomaterials and the associated release of heavy metal ions across an organic/aqueous interface and solar irradiation by taking PbS quantum dots as a model system. Using fluorescent metal ion sensors and steady-state fluorescence spectroscopy, we quantify the amount of Pb^{2+} ions released by photochemical etching of PbS quantum dots.

Further, with the help of cytotoxicity assays, comet assays, and DNA gel electrophoresis, we investigate the adverse effects of photoetched nanoparticles and the released metal ions to cultured cells. These studies reveal DNA damage as well as cell proliferation after exposure of cells to metal ions released from the nanoparticles. Nevertheless, the cytotoxicity Pb^{2+} ions are less than that caused by Cd^{2+} ions released from CdSe quantum dots. Further studies in various cell lines and animal models are needed for critically understanding the health and environmental effects of using greater amounts of heavy metal-based engineered nanomaterials.

Keywords:, quantum dots, engineered nanomaterials, cytotoxicity, genotoxicity, nanoparticles

Introduction

There is growing interest in understanding the cytotoxicity of engineered nanomaterials that are increasingly used in a variety of applications including energy harvesting, optoelectronic devices, bioanalysis, and therapeutic, diagnostic and cosmetic applications.[1-3] Engineered nanomaterials are designed with physical properties tailored by composition, size, and surface coatings that affect the toxicity of the material.[4-7,45,46] Advances in solar energy harvesting and optoelectronic devices have lead researchers to use transition metals[8-11] and chalcogenide nanomaterials such as AB, (where A = Cd, Hg, Pb, Cu, Zn and B = S, Se, Te)[12-15] as active components in devices. In particular, lead-based nanomaterials, such as lead and copper-based chalcogenide nanocrystals have attracted attention due to their strong quantum confinement, large exciton Bohr radius, and the large size-dependent tunable optical band gaps extending from the near infrared to the visible spectrum.[8-15] Since there are growing applications for these materials, there are concerns about the release of metal ions into the environment. These releases are in addition to waste runoff from mining operations and factories that make or refine lead, copper and other heavy metals.[16] These metals also enter the environment through waste dumps, waste-water

sludge digesters, industrial processes, and natural sources including wildfires, volcanoes and dust storms.[17-20] In addition to these natural sources and the current industrial production for devices that are known, greater amounts of lead and copper based nanoparticles are expected to be produced over the next 20 years for a diverse array of new nanotechnological applications. The disposal of these products will increase the exposure to heavy metals for the public. These nanomaterials are photoactive, and potentially could be transformed by photoetching, as observed with other semiconducting nanoparticles.[21-23] Thus, it is critical to quantify the amounts of metal ions released from heavy metal-based nanoparticles during exposure to solar simulated irradiation.

The toxicity of heavy metals such as lead are generally associated with neurotoxicity,[24,25] hepatotoxicity[26,27] and nephrotoxicity.[28,29] The specific differences in toxicity of these metal ions may be related to differences in solubility, transport, chemical reactivity and complexes with biomolecules formed within the body. Metal ions generally exert toxicity through interaction with cellular redox regulation/oxidative stress, interaction with DNA repair enzymes, and deregulation of cell proliferation.[30,31,44] The U.S. Department of Health and Human Services (HHS) has determined that lead compounds are human carcinogens based on limited evidences from studies in humans.[32] On the basis of sufficient evidence from animal studies, the US Environmental Protection Agency (EPA) has determined that lead is a probable human carcinogen.[33-35] Further, the International Agency for Research on Cancer (IARC) has determined that inorganic lead is a probable carcinogen to humans.[36] Although mutagenicity studies in microorganisms have yielded mostly negative results for lead, it is a clastogenic agent, as shown by the induction of chromosomal aberrations, micronuclei, and by sister chromatid exchanges in peripheral blood cells from lead workers.[37] However, studies of cancer in lead exposed workers have been inconclusive. Some nongenotoxic mechanisms that have been proposed for lead-induced cancer include the

inhibition of DNA synthesis and repair, alteration in cell-to-cell communication, and oxidative damage.[38,39]

Prior research into the toxicity of photodegraded engineered nanomaterials revealed the high degree of cytotoxicity and genotoxicity of Cd^{2+} ions released from Cd-based quantum dots.[40,41] This and the emerging applications of chalcogenide quantum dots and organometal halide perovskites spurred our interest to investigate the toxicity of Pb^{2+} ~~and Cu^{2+}~~ ions frequently used in such nanomaterials. This research revealed that Pb^{2+} ions can induce cytotoxic and genotoxic effects in human cells but are not as toxic as Cd^{2+} ions. As a comparison, the toxicities of Cu^{2+} ions were also evaluated. Copper is an essential element, required in the diet for maintaining good health, however excessive amounts of copper can produce toxic effects.[42,43] Such results are vital for assessing the risk to public health and what actions are required to effectively protect workers and consumers exposed to such nanomaterials.

Experimental Section

Materials and Methods

Preparation of nanoparticles

PbS and CuS quantum dots were prepared by the thermolysis of a lead or copper thiolate derived precursor as described by Sigman *et al*.[47] The PbS and CuS quantum dots were washed with deionized water and ethanol, before being dissolved in chloroform. Aqueous dispersions of both PbS and CuS quantum dots were prepared by the exchange of ligands with dihydrolipoic acid, which was according to a previous method used for preparing aqueous CdSe quantum dots.[48]

Solar simulated UV-irradiation of engineered nanomaterials:

Solar simulated UV irradiation was performed using a 75 W Xenon lamp equipped with a band-pass filter to allow UV-radiation (330 to 400 nm) to pass through. The intensity of excitation light was set to that of solar UV radiation at sea level by applying neutral density filters and adjusting the distance between the light source and the sample. Photoetching experiments were conducted to measure the amount of Pb^{2+} and Cu^{2+} ions leaching that occurs during the simulated solar UV irradiation. In the photoetching experiments, aqueous solutions of PbS or CuS nanoparticles were irradiated with ultraviolet light for intervals of 3, 6, and 9 hours. After each irradiation interval, the sample was loaded in a dialysis cassette for 2 kDa molecular weight cutoff, and dialyzed overnight by immersing in deionized water under vigorous stirring. The dialysis step was selected for separating ions from nanoparticles. Concentrations of Pb^{2+} and Cu^{2+} ions were estimated from the ions released into deionized water and the dilution factor. In separate experiments, 5 mL nanoparticle samples were exposed to solar simulated UV light and 1 ml samples were collected after each irradiation interval. Samples were stored in a dark bottle for quantifying the amount of ions produced and evaluating the cytotoxic effects of the leached ions.

Cell culture

We used human lung epithelial adenocarcinoma cells (H1650) for evaluating the cytotoxicity of metal ions leached out during the solar simulated UV irradiation of PbS and CuS nanoparticles. H1650 cells were cultured up to ~ 60 % confluence in DMEM medium supplemented with 10% heat-inactivated fatal bovine serum (FBS) and penicillin/streptomycin (P/S) under humidified 5% CO_2 atmosphere at 37°C. For further evaluation on the neurotoxicity of lead, rat pheochromocytoma (PC12) cells were used in addition to H1650 cells. PC12 cells were cultured up to ~ 90 % confluence in DMEM medium supplemented with 5% heat-inactivated fatal bovine serum (FBS), 5% horse serum (HS) and 1% P/S under humidified 5% CO_2 atmosphere at 37°C.

Cell viability (MTT) assay

The protocol for 3-(4,5-dimethylthiazol-2-yl)-2,5-diphenyltetrazolium bromide (MTT) assay was supplied by the manufacturer (Cell Proliferation Kit I (MTT), Merck, USA). Details of MTT assay are provided elsewhere.[50] Briefly, H1650 or PC12 cells were seeded onto 96 well clear bottom plates and cultured up to 90% confluence. The cells were washed with PBS and the medium was replaced with a medium containing Pb^{2+} or Cu^{2+} ions, PbS or CuS quantum dots, or the photo-irradiated solutions of PbS or CuS quantum dots. The cells were then incubated with the metal ion or quantum dot samples for 4 or 72 hours and washed with PBS. Successively, the medium was replaced with DMEM supplemented with the serums containing MTT, and the cells were incubated overnight. Finally, the cells were treated with the lysis buffer provided in the MTT assay kit and incubated overnight, during which the crystals of formazan, which was formed from MTT, were dissolved into a purple solution. The optical density of formazan formed as a result of the reduction of MTT by the NADP/H-dependent oxidoreductase enzymes in the cytosol was estimated using a microplate reader (Multiskan Sky TCD, ThermoFisher, USA) with recording The results were analyzed statistically using Igor Pro v6.3 using a one-way ANOVA with a Dunnett's post *hoc* test for significance.absorbance at 570 nm.

Comet genotoxicity assay

Reagents including the lysis solution, alkaline unwinding solution, alkaline electrophoresis solution and staining solution were prepared per the protocol for the CometAssay® Kit (Trevigen, MD, USA) provided by the manufacturer. H1650 or PC12 cells were cultured up to 80 %

confluency and then cultured in the presence or absence of Pb^{2+} or Cu^{2+} ions from $PbCl_2$ for 72 hrs. The cells were harvested by applying trypsin, and washed with PBS, and collected into pellets by centrifugation (500 g, 3 min). In parallel, low molecular weight agarose (LMAgarose) was heated at 95°C and successively stabilized at 37°C for 20 min. The cell pellets were suspended separately in 500 μL PBS, mixed with LMAgarose at a 1:10 (v/v) ratio, and immediately pipetted onto the comet slide glass. The agarose coated slides were allowed to gel in the dark at 4°C for 15 minutes, followed by soaking the gel in chilled lysis solution for overnight. The slides were then soaked in an alkaline chromosome/DNA unwinding solution for 30 minutes at room temperature in the dark. The slides were placed in the pre-chilled alkaline electrophoresis solution in an electrophoresis apparatus and gel electrophoresis was performed by applying 21 volts, 30 mA for 45 minutes. The slides were then immersed twice in deionized water for 5 minutes and then in 70% ethanol aqueous solution before drying at 44°C for 15 minutes. DNA in the slides were stained with Syto16 dye (Invitrogen, USA) by pipetting 10 μM dye solution onto the dried agarose. The stained slides were placed in the refrigerator for 5 minutes, excess dye solution was gently pipetted out and the slides were dried at room temperature in the dark. Samples are stored in a desiccator until imaging using fluorescence microscopy. Comets were observed by a fluorescence microscopy and scored using a imaging software (Adobe Photoshop, Adobe, USA) with evaluating the area and fluorescence intensities of the comet cores and tails respectively.

Steady-state absorption and fluorescence spectroscopy

Absorption and fluorescence spectra were recorded using an Evolution 201/220 spectrophotometer (Thermo Scientific. USA). Fluorescence spectra were recorded using a Hitachi-F-4500 spectrofluorometer (Hitachi, Japan). Samples for fluorescence measurements were excited at 415 nm. Fluorescence detections of Pb^{2+} and Cu^{2+} ions were carried out using solutions

of 5,10,15,20-tetrakis (4-carboxyphenyl) porphyrin (TCPP) (20 nM in 5% K_2CO_3 solution) or the commercial Measure iT Pb/Cd sensor dye (Thermo Scientific. USA) by adding 50 µL solutions of $CuSO_4$ or $Pb(NO_3)_2$ or photo-irradiated PbS or CuS quantum dots (concentrations of standards $Pb(NO_3)_2$, ranged from 100 uM to 1 mM).

Atomic force microscopy (AFM) imaging

Samples for AFM imaging were prepared by using colloidal solutions of PbS quantum dots, depositing the solutions onto freshly cleaved mica sheets and drying in air. AFM images were taken with an MFP-3D AFM (Asylum Research, Santa Barbara, USA) equipped with reflective aluminum-coated ultra-sharp (radius of curvature ~ 10 nm) silicon nanoprobes (Olympus, Japan). We used cantilevers having 160 μm long, a spring constant of ca 42 N/m, and a resonance frequency of ~ 360 kHz. Here, AFM images were collected in the tapping mode in air, and the average diameters of the particles were estimated from the height image.

Results and Discussion

Prior to solar simulated photo-irradiation, the PbS quantum dots were characterized by atomic force microscopy (AFM). The size distribution of measurements taken from the AFM height images showed an average diameter of ca. 3 nm (Fig. 1A) for the PbS nanoparticles. This is usual distribution and diameter for the nanoparticles.[47] Using a tapping mode AFM, a 3-D image of PbS quantum dots was created as seen in Fig. 1B.
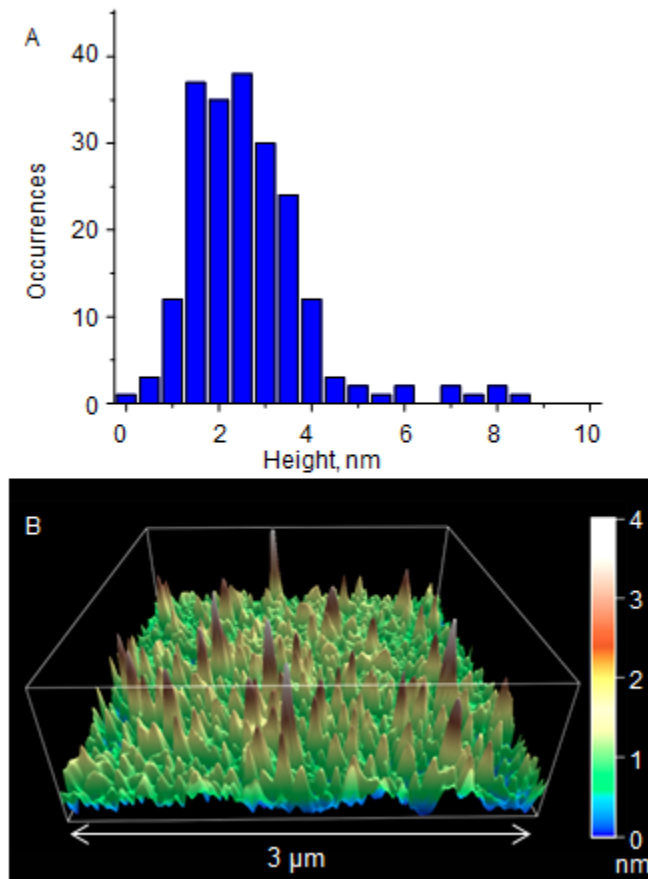
Figure 1. (A) Size distribution of PbS quantum dots from AFM height measurements and (B) 3D AFM image of PbS quantum dots deposited on a freshly cleaved mica sheet.

UV-absorption spectroscopy shows that PbS quantum dots show prominent absorption of light in the UV region prior to photo-irradiation with an increase in absorbance after prolonged photo-irradiation time, which is due to light scattering by particle aggregates formed as a result of degradation of surface ligands (Supporting information). The degradation of quantum dots and the release of Pb^{2+} ions after photo-irradiation were examined using fluorescence spectroscopy. Here Measure iT Pb/Cd ion sensor dye and 5,10,15,20-tetrakis (4-carboxyphenyl) porphyrin (TCPP) were selected to be the scavenger and sensor of the ions released. Previous studies showed that the fluorescence of the porphyrin molecules is sensitive to divalent metal ions including Hg^{2+}, Cd^{2+}

and Zn^{2+} ions due to the coordination of metal ions to the porphyrin ring.[51] Thus we first tested the detection of externally added Pb^{2+} ions using TCPP to observe if Pb^{2+} ions would quench the fluorescence by forming a non-fluorescent complex with TCPP. As seen in Fig. 2A, TCPP fluorescence is quenched upon addition of the 1 mM $Pb(NO_3)_2$ solution. The concentration of Pb^{2+} ions was varied in the range of 100 μM to 1mM, to measure the Pb^{2+} detection range of the TCPP sensor. As seen in Fig. 2B, the fluorescence quenching of TCPP does not follow linear relationship with the concentration of $Pb(NO_3)_2$ added, suggesting that TCPP cannot be used for the quantification of Pb^{2+} ions released from photo-irradiated PbS quantum dots. Instead, the fluorescence gradually decreased with elapse of time after the addition of Pb^{2+} ions, which was independent of the concentration of Pb^{2+}ions. Further, gradual precipitation of TCPP-Pb^{2+} complex was observed with time.Thus, we rely on the commercial Measure iT Pb/Cd ion sensor dye for quantitative detection of Pb^{2+} ions released from photo-irradiated PbS quantum dots. The release of Pb^{2+} ions and detection of the ions are schematically presented in Fig. 2C. The structures of TCPP before and after the binding to lead are shown in Fig. 2C and 2D, respectively.
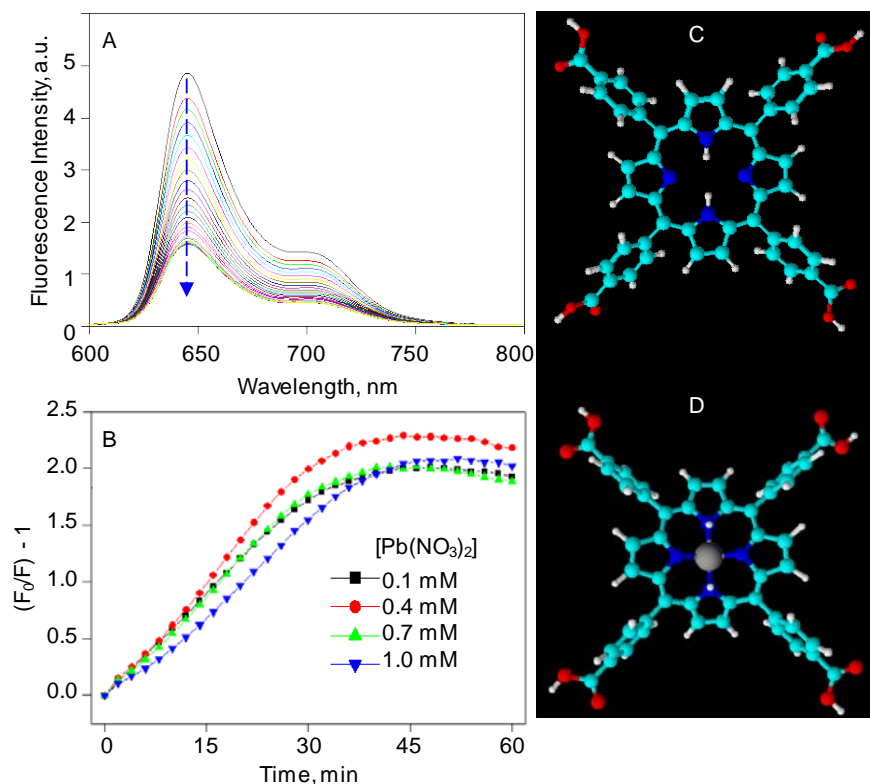
Figure 2. (A) Fluorescence spectra of TCPP after addition of 1mM solution of Pb(NO$_3$)$_2$. (B) Time-dependent fluorescence intensities of TCPP solutions after the addition of Pb^{2+} ions from solutions of PbNO$_3$. (C,D) Molecular structures of TCPP (C) without and (D) with lead.

To quantitatively detect Pb^{2+} released from photoactivated quantum dots, we employed the commercial fluorescence sensor Measure iT Pb/Cd ion sensor. As shown in Fig. 3B, the fluorescence of the sensor sensitively enhances with increase in the concentration of externally added Pb^{2+} ions. The sensor efficiently and quantitatively detects Pb^{2+} ions in solution at sub-micromolar concentration levels. The Stern-Volmer plot of fluorescence is shown in the inset with an equation, $y = 4.004x + 0.3523$, $R^2 = 0.9962$. By using the fluorescence enhancement factors of Measure iT dye obtained for Pb^{2+} in Pb(NO$_3$)$_2$ solutions having known concentrations, we estimate the fluorescence enhancement factor for Pb^{2+} ions leached out from PbS quantum dots. Here, the ratio of Measure iT sensor dye to Pb^{2+} ions was set for maximum fluorescence sensitivity by

measuring the fluorescence intensity of the dye in presence of 5 nM solution of $Pb(NO_3)_2$. As seen in Fig. 3C (green trace), there is a detectable amount of Pb^{2+} ions measured after three-hour photo-irradiation of PbS; however, for zero, six and nine hours, there were essentially no Pb^{2+} ions detected. The minimum concentration of Pb^{2+} ions to show a significant amount of fluorescence enhancement by the Measure iT sensor dye was 5 nM, whereas for smaller amounts added, a consistent, reproducible increase was not observed. Thus, the amount of free Pb^{2+} ions present in a solution of as-prepared PbS quantum dots is below 5 nM. However, with time under irradiation up to 3 hours, appreciable amounts (ca 80 nM) of Pb^{2+} ions were released from PbS quantum dots (Fig. 3A and 3C). This release is due to surface etching of photoactivated PbS. However, the release of ions was below the detectable level (5 nM) beyond 3 hours, which suggests that photo-etching cannot completely degrade PbS quantum dots, and aggregation of PbS after the release of dihydrolipoic acid (DHLA) ligands would happen. In other words, PbS quantum dots are stabilized by aggregation after the release of surface ligands and a definite amount of Pb^{2+} ions. It is to be investigated that the effect and efficiency for the aggregation by different types of ligands from DHLA.
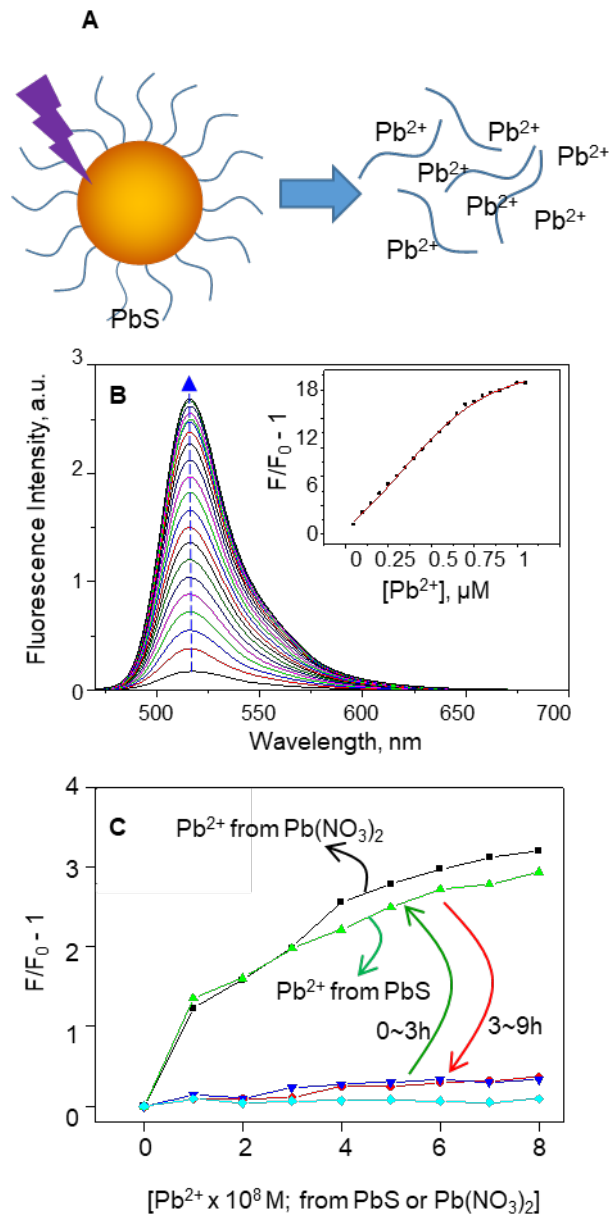
Figure 3. (A) Schematic presentation of UV induced release of ligands and metal ions from PbS quantum dots, (B) Fluorescence spectra of the Measure iT dye after addition of solution of Pb^{2+} solution; inset: Stern-Volmer plot. . (C) Fluorescence enhancement factors of Measure iT for Pb^{2+} ions released from PbS quantum dots under solar-simulated UV irradiation for 0 to 3, 3 to 6, and 6 to 9 h.

   As comparison experiments, the series of experiments using Cu^{2+} ions were performed instead of using Pb^{2+}. The absorption and fluorescence spectral measurements demonstrated a similar trend to that of Pb^{2+}. To detect the release of Cu^{2+} ions from photodegraded CuS quantum dots, we first

employed TCPP as the metal ion sensor. As observed in Fig. 4A, TCPP fluorescence is decreased to a small extent after the addition of Cu^{2+} ions (0.1 mM solution of $CuCl_2$). When compared with fluorescence quenching of TCPP by Pb^{2+} ions, the fluorescence of TCPP was rather insensitive to Cu^{2+} ions added (Fig. 4A). This result suggest that TCPP is not a suitable fluorescence probe for trace amounts (sub-micromolar concentrations) of Cu^{2+} ions released from CuS. Here the concentration of Cu^{2+} ions can be low due to the dilution (ca 10^{-2}) as a result of dialysis. To suppress the dilution factor in the detection of Cu^{2+} ions released from photoactivated CuS quantum dots, the photoactivated CuS solution was directly added to a solution of TCPP, and the fluorescence spectra of TCPP were recorded. Surprisingly, the addition of solutions of photoetched CuS nanoparticles resulted in the fluorescence enhancement of TCPP (Fig. 4B and 4C). To confirm if the enhancement was due solely to the Cu^{2+} ions, solutions (sub-millimolar to nanomolar) of $CuSO_4$ or $CuCl_2$ were added to TCPP solutions. However, we did not detect any fluorescence enhancement for TCPP in the presence of Cu^{2+} ions. Thus, the fluorescence enhancement, although minor, observed after addition of photoactivated CuS quantum dots to TCPP is attributed to the adsorption of TCPP to the surface of CuS and the energy transfer from CuS to TCPP (Fig. 4C). These experiments were repeated by replacing TCPP with the commercial Measure iT sensor dye. In contrast with an enormous (ca 400%) enhancement of fluorescence intensity of the sensor in the presence of sub micromolar concentrations of Pb^{2+} ions as well as photoactivated PbS quantum dots, the fluorescence intensity increased only 30% in the presence of photoactivated CuS quantum dots (Fig. 4D). Also, the fluorescence of the sensor was less sensitive to externally added Cu^{2+} ions ($CuSO_4$ or $CuCl_2$ solution). These results show neither TCPP nor Measure iT is capable of detecting Cu^{2+} ions. The slight (ca 30%) enhancement of fluorescence intensity of Measure iT, which is comparable to that of TCPP, indicates energy

transfer from CuS to the sensor. While the main focus of this research is to detect release of ions from PbS quantum dots and evaluate toxic effects of Pb^{2+} ions released, evaluation and comparing methodology of Cu^{2+} with Pb^{2+} is to be investigated.
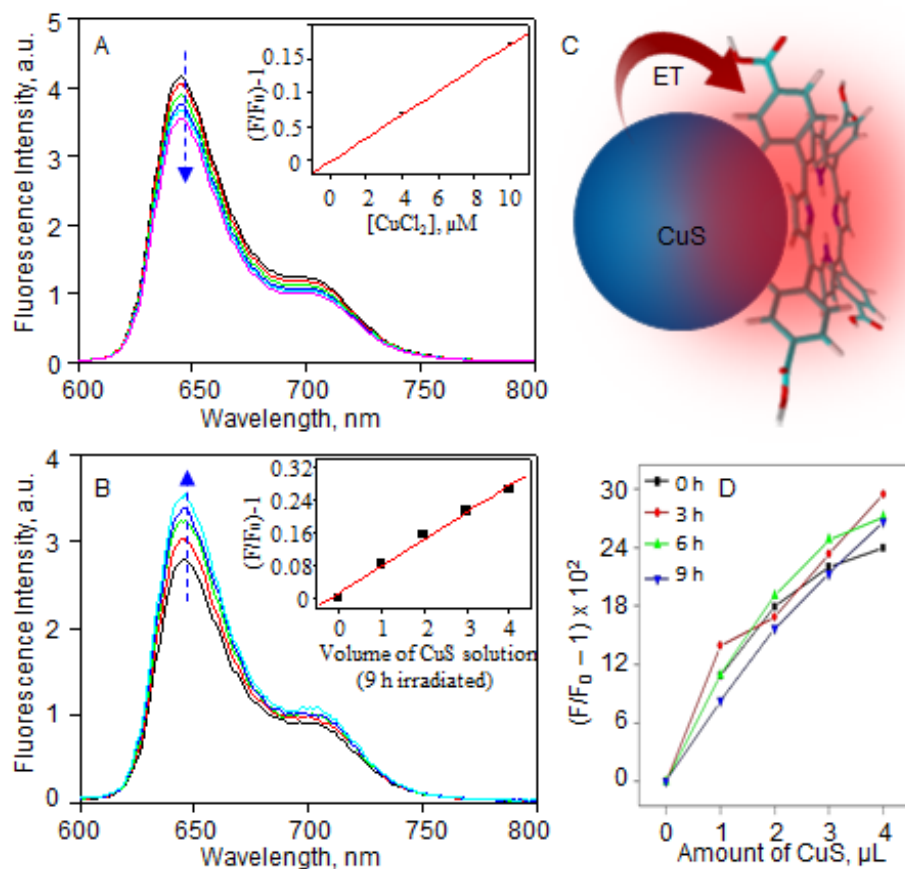

Figure 4. (A) Fluorescence spectra of TCPP with addition of Cu^{2+} originated from $CuSO_4$; inset: Stern-Volmer plot. (B) Fluorescence spectra of TCPP after addition of CuS nanoparticle after 9 hr UV irradiation; inset: Stern-Volmer plot. (C) Graphical presentation of energy transfer from CuS quantum dots to TCPP. (D) Fluorescence intensity traces of Measure iT sensor dye in presence of photoactivated CuS quantum dots.

To investigate the toxicity of environmentally transformed PbS and CuS quantum dots, we treated human lung epithelial adenocarcinoma (H1650) cells with quantum dots before and after solar simulated UV irradiation for 3 to 9 hours and examined the cytotoxic effects and genotoxic

effects by the MTT and comet assays. H1650 cells were chosen because they were often used for evaluating nanomaterials in the literature.[51] As shown in Fig. 5B and 5C, we observed slight (ca. 12~15%) proliferative effects on H1650 cells by both PbS and CuS quantum dots and irradiated for 6 hours or longer. The degree of proliferation is obtained by comparing the MTT assay results for H1650 cells without or with Pb^{2+} or Cu^{2+} ions treatment (Fig 5A). The proliferative effects induced by DHLA-capped PbS and CuS quantum dot solutions, although minor, is comparable to the results obtained for DHLA-capped CdSe, CdSe/ZnS and ZnO quantum dots.[52] The proliferation can be attributed to suppression of intrinsic cytotoxicity by DHLA ligands released from the surface of quantum dots.[52]

Lead is a major environmental toxin that causes hematological, gastrointestinal and neurological dysfunction.[32] To obtain further insight into the toxicity of PbS, we analyzed long-term MTT assay results for H1650 cells treated with Pb^{2+} ions and Cu^{2+} ions solutions having concentrations equivalent or higher than that released from quantum dots (Fig. 5D and 5E). As shown in Fig. 5D, there is virtually no decrease in viability of cells exposed to Pb^{2+} or Cu^{2+} ion solutions having concentrations as high as 100 µM, which is more than 3 orders of magnitude higher in centration than that released from PbS or CuS quantum dots.
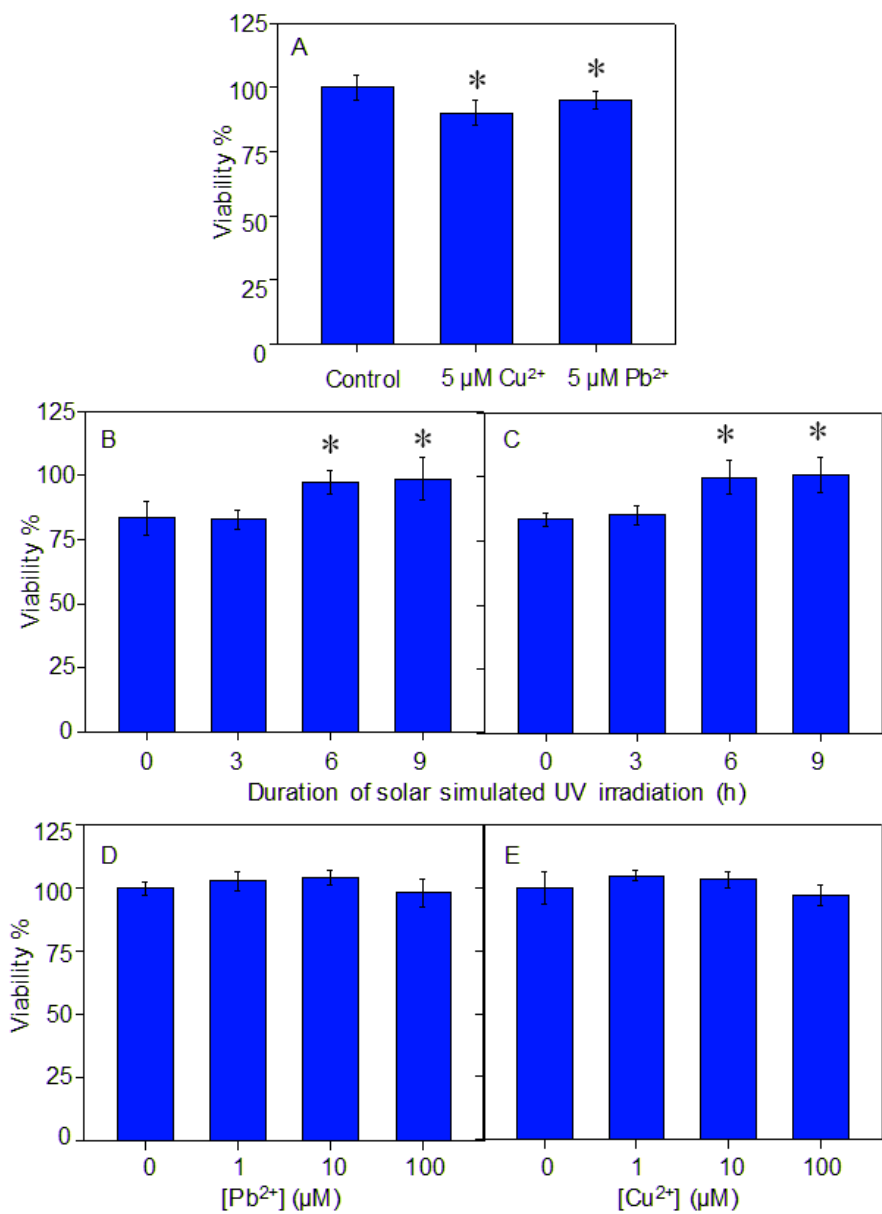
Figure 5. Cell viabilities of H1650 cells treated with PbS quantum dots, CuS quantum dots Pb^{2+} originated from $PbCl_2$ and Cu^{2+} originated from $CuCl_2$. Statistically significant differences between the negative control and each condition are illustrated with asterisks (*$P < 0.05$) (A) H1650 cells treated with Pb^{2+} and Cu^{2+} for 72 hr. (B, C) H1650 cells treated with solutions of the photoetched (B) PbS quantum dots and (C) CuS quantum dots. (D, E) Cells treated with different concentrations of (D) Pb^{2+} and (E) Cu^{2+} ion solutions.

Genotoxicity of Pb^{2+} ions was further investigated using the comet assay and agarose gel electrophoresis. Here we treated H1650 cells, PC12 cells as model nerve cells, or Calf thymus DNA. The comet assay of Pb^{2+} ions reveals only low levels of DNA damage and only a few extensively damaged comets were found (Fig. 6A). Such results seem somewhat surprising, since lead is widely recognized as an environmental pollutant, and its presence in the environment is strictly regulated. The results of H1650 cells showed only slight comet tail formation with low percentages of DNA in the tail as well as shorter comet lengths. Results show that most comets scored low amounts of damage and only a few highly damaged nuclei were formed. Thus, genotoxicity of Pb^{2+} ions is extremely low, compared to H1650 cells similarly exposed to Cd^{2+} ions.[41] The comet assay was also utilized to investigate genotoxicity of Cu^{2+} ions released from CuS quantum dots. As seen in Fig. 6B, cells exposed to Cu^{2+} ions show similar genotoxicity, as compared to cells exposed to Pb^{2+} ions. The percent DNA in the tail formed for Pb^{2+} and Cu^{2+} ion comet assays are shown together in Fig. 6D to compare the DNA damaging potential of each ion with earlier results using Cd^{2+} ions. As seen in Fig. 6D, Cd^{2+} ions caused significantly more DNA damage than Pb^{2+} and Cu^{2+} ions. The DNA comet assay results for both Pb^{2+} and Cu^{2+} ions (Fig. 6C) show no significant damage to DNA for either long-term or short-term incubation. These ions, however, are not completely non-toxic, since lead, for example, is known for its serious neurotoxicity - especially for children.[24] In particular, lead is damaging to developing brains and the removal of lead from paint is important for reducing lead exposure to children.[32] In contrast to lead, copper is an essential element incorporated into numerous metalloenymes involved in a variety of biomolecular functions including biosynthesis, protein formation, and antioxidant defenses.[42] The toxicity of lead was further assessed using PC12 cells, a known model for neurons. The results showed no significant acute ion toxicity to cell viability (Fig. 7A), but genotoxicity

with significant DNA damage (Fig. 7B). The relatively high values in the comet assay would reflect the high susceptibility of PC12 cells to cytotoxicity to lead.
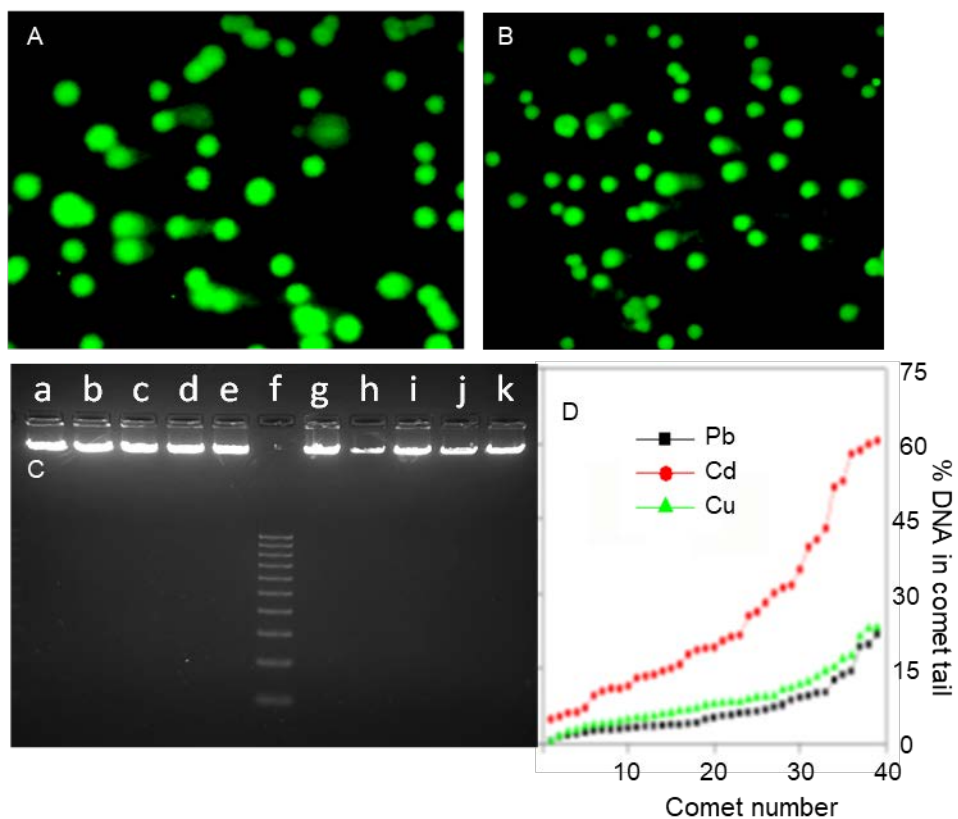

Figure 6. (A, B) Comet assay images of H1650 cells exposed to 5 μM solutions of (A) Pb^{2+} ions and (B) Cu^{2+}ions, both for 72 hr. (C) Gel electrophoresis picture of CT DNA: (a-e) long term (7 days) and short term (3 hr) incubations with (a,g) CuS, (b,h) Cu^{2+} ions. (c,i) PbS, (d,j) Pb^{2+} ions and (e,k) control; (f) DNA ladder. (C) Software-based comet score showing the percent DNA in the tail of H1650 cells exposed to Cd^{2+}, Pb^{2+} or Cu^{2+} ions (5 μM) for 72 hours.(D) Software-based comet score showing the percent DNA in the tail of H1650 cells exposed to Cd^{2+}, Pb^{2+} or Cu^{2+} ions (5 μM) for 72 hours.

Figure 7. Cell viability and neurotoxicity assays on PC12 cells. (A) MTT assay after the treatment of Pb^{2+} for 72 h. Statistically significant differences between the negative control and

each condition are illustrated with asterisks ($*P < 0.05$). (B) Software-based comet score showing the percent DNA in the tail of PC12 cells exposed to Pb^{2+} ions (0.1 µM) for 72 hours.

Summary

The toxicity of transition metal chalcogenide nanoparticles is an area of growing concern for health and occupational safety regulators. It is known that prolonged exposure to lead may cause reproductive impairment, hypertension, and nephropathy.[29]   Lead also slows nerve conduction, alters calcium homeostasis, inhibits enzymes and stimulates synthesis of binding proteins. Although major sources of toxic heavy metal exposure are dust, water, paint, cosmetics, folk remedies and food supplements,[32] increased production and use of transition metal nanoparticles need attention. In this study, it is shown that high levels of either Pb^{2+} or Cu^{2+} ions are not enough to produce severe cytotoxicity or genotoxicity as observed with Cd^{2+} ions. Previous researchers have reviewed the role of oxidative tissue damage and altered fatty acid composition in the toxicities of lead, and based on experimental evidences, oxidative mechanisms appear to be involved in some of the toxic effects of lead.[39] Thus further sub-lethal *in vitro* and *in vivo* assays of the oxidative stress induced by lead and other heavy metal ions released from nanoparticles are required to obtain a complete picture of the toxicity of nanomaterials.

Author contributions

All authors contributed substantially to the research. P.J.,M.V.,F.L. and V.B. framed the project; P.J.,R.K. and V.B. carried out nanoparticle preparation and fluorescence measurements; P.J. and V.B carried out AFM imaging; P.J.,S.S., J.S., Y.T., and V.B. carried out cytotoxic and genotoxic assays; and P.J., M.V. J.S., Y.T., and V.B. analyzed the data. All authors participated in the writing of the manuscript.

Competing interests: The authors declare no competing financial interests.

References

1.   Y. Zhu, X. Liu, Y. Hu, R. Wang, M. Chen, J. Wu, Y. Wang, S. Kang, Y. Sun and M. Zhu, *Environ. Res.*, 2019, **174**, 54–60.

2.   D. Wu, Y. Ma, Y. Cao and T. Zhang, *Sci. Total Environ.*, 2020, **702**, 134994.

3.   S. M. Geary, A. S. Morris and A. K. Salem, *J. Allergy Clin. Immunol.*, 2016, **138**, 405–408.

4.   S. Wang, F. Li, X. Hu, M. Lv, C. Fan and D. Ling, *Adv. Ther.*, 2018, **1**, 1800059.

5.   Jones, P. et al., *Nanoscale,* 2013, **5**, 9511-9516.

6.   G. V. Vimbela, S. M. Ngo, C. Fraze, L. Yang and D. A. Stout, *Int. J. Nanomedicine*, 2017, **12**, 3941–3965.

7.   P. N. Navya and H. K. Daima, *Nano Converg.*, 2016, **3**, 1–14.

8.   M. Xiao, F. Huang, W. Huang, Y. Dkhissi, Y. Zhu, J. Etheridge, A. Gray-Weale, U. Bach, Y. B. Cheng and L. Spiccia, *Angew. Chemie - Int. Ed.*, 2014, **53**, 9898–9903.

9.   Y. Deng, X. Zheng, Y. Bai, Q. Wang, J. Zhao and J. Huang, *Nat. Energy*, 2018, **3**, 560–566.

10.   J. H. Im, I. H. Jang, N. Pellet, M. Grätzel and N. G. Park, *Nat. Nanotechnol.*, 2014, **9**, 927–932.

11.   M. Zhong, Y. Liang, J. Zhang, Z. Wei, Q. Li and D. Xu, *J. Mater. Chem. A*, 2019, **7**, 6659–6664.

12.   W. Jang, Y. T. Kwon, H. R. Lim, Y. H. Choa and D. H. Wang, *Appl. Surf. Sci.*, 2019, **484**, 1253–1262.

13.   A. Kagkoura, T. Skaltsas and N. Tagmatarchis, *Chem. - A Eur. J.*, 2017, **23**, 12967–12979.

14.   X. Tong, X. Li, A. I. Channa, R. Liu, J.-Y. Xu, P. Yu, L. Chang, H. Ji, Q. Wang and Z. M. Wang, *Sol. RRL*, 2019, **3**, 1900186.

15.   Wang, F. et al., J. *Am. Chem. Soc.,* 2015, **137**, 12006-12012.

16.   D. Yu, L. Bai, J. Zhai, Y. Wang and S. Dong, *Talanta*, 2017, **168**, 210–216.

17.   X. He, X. Qiu, C. Hu and Y. Liu, *J. Dispers. Sci. Technol.*, 2018, **39**, 792–801.

18.   P. Biswas, C.Y. Wu, *J. Air Waste Manag. Assoc.*, 2005, **55**, 708-746.

19.   Y. Wu, H. Pang, Y. Liu, X. Wang, S. Yu, D. Fu, J. Chen and X. Wang, *Environ. Pollut.*, 2019, **246**, 608–620.

20.   V.L. Colvin, *Nature,* 2003, **21(10)**, 1166-1170.

21.   O. V. Chashchikhin and M. F. Budyka, *J. Photochem. Photobiol. A Chem.*, 2017, **343**, 72–76.

22.   T. Lee, K. Shimura and D. Kim, *Phys. Chem. Chem. Phys.*, 2018, **20**, 11954–11958.

23.   Y. T. Shen, D. Lei and W. Feng, *J. Mater. Chem. C*, 2013, **1**, 1926–1932.

24.   Y. Wu, Y. Wang, M. Wang, N. Sun and C. Li, *Toxicol. Ind. Health*, 2017, **33**, 332–339.

25.   A. Nan, L. Chen, N. Zhang, Z. Liu, T. Yang, Z. Wang, C. Yang and Y. Jiang, *Arch.*

Toxicol., 2017, **91**, 1671–1684.

26. M. Labudda, 2013, **64**, 565–568.

27. S. Pantic, S. Radojevic Skodric, Z. Loncar and I. Pantic, *Rev. Adv. Mater. Sci.*, 2019, **58**, 201–205.

28. L. V. Puchkova, A. N. Skvortsov, P. Rusconi, E. Y. Ilyechova and M. Broggini, *BioMetals*, 2016, **29**, 841–849.

29. Q. Jia, X. Ha, Z. Yang, L. Hui and X. Yang, *Toxicol. Mech. Methods*, 2012, **22**, 705–710.

30. D. Beyersmann, and A. Hartwig, *Arch. Toxicol.,* 2008, **82**, 493-512.

31. D. M. Templeton, *Toxics*, 2015, **3**, 170–186.

32. Agency for Toxic Substances and Disease Registry, *Atlanta*, 2007, GA.

33. Silbergeld, E. K. et al., Am. *J. Ind. Med.*, 2000, **38**, 316-323.

34. NTP. 2005. Report on Carcinogens. 11th Ed. Research Triangle Park, NC: U.S. Department of Health and Human Services, National Toxicology Program.

35. IRIS. 2005. Lead. U.S. Environmental Protection Agency. Washington, DC: Integrated Risk Information System.

36. World Health Organization International Agency for Research on Cancer. (2004). IARC monographs on the evaluation of carcinogenic risks to humans, inorganic and organic lead compounds. Lyon, France, IARC, **87.**

37. F.Y. Wu et al., *Cancer Epidemiol. Biomarkers Prev*., 2002, **11**, 287-290.

38. C. F. Lu, X. Y. Yuan, L. Z. Li, W. Zhou, J. Zhao, Y. M. Wang and S. Q. Peng, *Ecotoxicol. Environ. Saf.*, 2015, **122**, 537–544.

39. N. Pawlas, E. Olewinska, I. Markiewicz-Górka, A. Kozlowska, L. Januszewska, T. Lundh, E. Januszewska and K. Pawlas, *Adv. Clin. Exp. Med.*, 2017, **26**, 939–945.

40. Y. Fujiwara, C. Yamamoto, E. Yoshida, Y. Kumagai and T. Kaji, *Arch. Toxicol.*, 2016, **90**, 259–267.

41. R. Jindal and S. Verma, *Ecotoxicol. Environ. Saf.*, 2015, **118**, 1–10.

42.   D. Denoyer, S. Masaldan, S. La Fontaine and M. A. Cater, *Metallomics*, 2015, **7**, 1459–1476.

43.   T. E. Henson, J. Navratilova, A. H. Tennant, K. D. Bradham, K. R. Rogers and M. F. Hughes, *Nanotoxicology*, 2019, **13**, 795–811.

44.   Horie, M. et al. (2012). In Vitro Evaluation of Cellular Response Induced by Manufactured Nanoparticles. *Chem. Res. Toxicol.* **25**, 605-619.

45.   Derfus, A. M. et al. (2004). Probing the Cytotoxicity of Semiconductor Quantum Dots. *Nano Lett.* **4**, 11-18.

46.   Hoshino, A. et al. (2004). Physicochemical Properties and Cellular Toxicity of Nanocrystal Quantum Dots Depend on their Surface Modification. *Nano Lett.* **4**, 2163-2169.

47.   M. B. Sigman, A. Ghezelbash, T. Hanrath, A. E. Saunders, F. Lee and B. A. Korgel, *J. Am. Chem. Soc*., 2003 **125**, 16050-16057.

48.   H. T. Uyeda, I. L. Medintz, J. K. Jaiswal, S. M. Simon and H. Mattoussi, *J. Am. Chem. Soc.,* 2005, **127**, 3870-3878.

49.   V. C. Nair, C. Muthu, A. L. Rogach, R. Kohara and V. Biju., *Angew. Chem. Int. Ed.* 2016, **55**, 1-6.

50.   G. Fotakis, and J. A. Timbrell, *Toxicology Letters,* 2006, **160**, 171-177.

51.   Biju et al., *Nanoscale*, 2013, **5**, 9511-9516.

52.   R. A. Hardman, *Environ. Health Perspect*., 2006, **114**, 165-172.